

# Polymethylaluminoxane supported zirconocene catalysts for polymerisation of ethylene

Thomas A. Q. Arnold, Zoë R. Turner, Jean-Charles Buffet and Dermot O'Hare\*

Chemistry Research Laboratory, University of Oxford, 12 Mansfield Road, OX1 3TA, Oxford, UK.

Corresponding author: dermot.ohare@chem.ox.ac.uk

## ABSTRACT

We report here the synthesis of two new ansa-bridged permethylindenyl zirconocenes, their reaction with solid polymethylaluminoxane (sMAO) and their use in slurry phase ethylene polymerisation. *Meso*-(EBI\*)Zr(CH<sub>2</sub>Ph)<sub>2</sub> and *meso*-(EBI\*)Zr(CH<sub>2</sub><sup>t</sup>Bu)Cl, (EBI\* = ethylenebis[1-(2,3,4,5,6,7-hexamethylindenyl)]) were synthesised from *meso*-(EBI\*)ZrCl<sub>2</sub> and K(CH<sub>2</sub>Ph) and K(CH<sub>2</sub><sup>t</sup>Bu) respectively. The new zirconocenes were characterised by NMR spectroscopy and X-ray crystallography, and density functional theory calculations were carried out. Solid precatalysts were obtained when these compounds were reacted with the polymethylaluminoxane support. Ethylene polymerisation activities of up to 6000 kg<sub>PE</sub>/mol<sub>Zr</sub>/h/bar were obtained in slurry polymerisation of ethylene. The polyethylenes showed molecular weights, *M<sub>w</sub>*, above 200 000 kg/mol and low polydispersities, *M<sub>w</sub>*/*M<sub>n</sub>* < 3.

**Keywords:** Polymethylaluminoxane, Zirconocene, Ethylene, Permethylindenyl, Polymerisation.

## 1. Introduction

Group 4 metallocenes were discovered by Wilkinson and Birmingham in 1954,[1] and have recently been investigated for N<sub>2</sub> binding and functionalisation,[2-3] as FLPs capable of activating small molecules such as CO<sub>2</sub> and H<sub>2</sub>,[4-6] and for  $\alpha$ -olefin polymerisation.[7]

The polymerisation of ethylene is industrially significant with annual production in excess of 75 million tonnes.[7] It has also been a topic of academic importance and the focus of a number of reviews.[8-11] Slurry phase polymerisation (both Ziegler Natta or single-site type) is an extremely important aspect of the industrial polymerisation

market.[11-13] For the immobilisation of single-site catalysts, the most commonly employed support material is silica but other inorganic materials such as zeolites and clays have also been investigated. Clays are typically ion exchanged, often with ammonium salts, before surface activation with alkylaluminium reagents.[14] They have also been employed by Suga and co-workers as supports for zirconocenes,[15] and were reported as active supports for Ziegler catalysts.[16,17]

We recently reported the use of silica,[18] aqueous miscible organic layered double hydroxide- (AMO-LDH),[18-20] and core shell@LDH-supported indenyl metallocenes,[21] for the slurry polymerisation of ethylene. Furthermore, we demonstrated that a catalyst based on a tungsten imido complex supported on solid polymethylaluminoxane (sMAO) was much more active and selective for the dimerisation of ethylene than the silica and AMO-LDH analogues.[22a] Very recently, we observed that an sMAO-supported permethylpentylene zirconium complex ( $\text{Pn}^*\text{ZrCp}^{\text{Me}}\text{Cl}_{\text{sMAO}}$ ) was superior in ethylene polymerisation activity relative to ssMAO and AMO-LDH-MAO (5.3 and 2.3 times respectively). Significantly, the slurry-phase ethylene polymerisation activities using equivalent complexes supported on sMAO demonstrated enhanced performance compared to the solution phase.[22b]

Here we report the synthesis and characterisation of two new ansa-bridged permethylindenyl zirconocene alkyl complexes, and the preparation of solid polymethylaluminoxane-supported complexes for evaluation of slurry phase ethylene polymerisation capability.

## 2. Materials and methods

### 2.1. General considerations

All reactions, unless specified otherwise, were performed under an atmosphere of nitrogen, using standard Schlenk techniques on a dual vacuum/inert gas manifold or within an MBraun UNIlab glovebox. Pentane, hexane, toluene and benzene were dried using an MBraun SPS-800 solvent purification system, stored in ampoules over a potassium mirror and degassed prior to use. Dichloromethane was stored over molecular sieves. Tetrahydrofuran was distilled from purple sodium/benzophenone ketyl radical and stored on molecular sieves. Benzene- $d_6$  (99.6%, Sigma Aldrich) and was dried over Na/K. Tetrahydrofuran- $d_8$  (99.6%, Goss Scientific) was dried over calcium hydride. All deuterated solvents were vacuum transferred and freeze-pump-thaw degassed three times prior to use.

Molecular sieves (3 Å, 8-12 mesh) were supplied from Acros Organics and were baked at 140 °C under vacuum ( $< 10^{-2}$  mbar) for at least six hours before use.

## 2.2. Complex syntheses

### 2.2.1. Preparation of *meso*-(EBI\*)Zr(CH<sub>2</sub>Ph)<sub>2</sub>

Benzene (50 mL) was added to a Schlenk tube containing *meso*-(EBI\*)ZrCl<sub>2</sub> (600 mg, 1.03 mmol) and K(CH<sub>2</sub>Ph) (295 mg, 2.27 mmol) and the reaction mixture was stirred for 18 h. Extraction with hexane (2 × 80 mL) and removal of the volatiles *in vacuo* afforded *meso*-(EBI\*)Zr(CH<sub>2</sub>Ph)<sub>2</sub> as a yellow solid in 64% yield (459 mg, 0.66 mmol). Single crystals were grown from a concentrated solution of hexane at −35 °C. <sup>1</sup>H NMR (400 MHz, 23 °C, benzene-*d*<sub>6</sub>): δ −0.70 (s, 2H, PhCH<sub>2</sub>), 1.83 (s, 2H, PhCH<sub>2</sub>), 1.85 (s, 6H, Cp-Me), 2.01 (s, 6H, Ar-Me), 2.04 (s, 12H, Cp/Ar-Me), 2.41 (s, 6H, Ar-Me), 2.50 (s, 6H, Ar-Me), 3.07 (m, 3.02-3.13, 2H, CH<sub>2</sub>), 3.67 (m, 3.62-3.73, 2H, CH<sub>2</sub>), 6.39 (d, <sup>3</sup>*J*<sub>HH</sub> = 7.5 Hz, 2H, *o*-Ph), 6.58 (d, <sup>3</sup>*J*<sub>HH</sub> = 7.5 Hz, 2H, *o*-Ph), 6.80 (t, <sup>3</sup>*J*<sub>HH</sub> = 7.2 Hz, 1H, *p*-Ph), 6.95 (t, <sup>3</sup>*J*<sub>HH</sub> = 7.3 Hz, 1H, *p*-Ph), 7.04 (t, <sup>3</sup>*J*<sub>HH</sub> = 7.6 Hz, 2H, *m*-Ph), 7.16 (t, <sup>3</sup>*J*<sub>HH</sub> = 7.6 Hz, 2H, *m*-Ph). <sup>1</sup>H NMR (400 MHz, 23 °C, tetrahydrofuran-*d*<sub>8</sub>): δ −1.01 (s, 2H, PhCH<sub>2</sub>), 1.60 (s, 2H, PhCH<sub>2</sub>), 2.04 (s, 6H, Cp-Me), 2.13 (s, 6H, Ar-Me), 2.15 (s, 6H, Ar-Me), 2.16 (s, 6H, Cp-Me), 2.39 (s, 6H, Ar-Me), 2.60 (s, 6H, Ar-Me), 3.44 (q, <sup>2</sup>*J*<sub>HH</sub> = 6.8 Hz, <sup>3</sup>*J*<sub>HH</sub> = 6.2 Hz, 2H, CH<sub>2</sub>), 3.92 (q, <sup>2</sup>*J*<sub>HH</sub> = 6.3 Hz, <sup>3</sup>*J*<sub>HH</sub> = 6.2 Hz, 2H, CH<sub>2</sub>), 6.07 (d, <sup>3</sup>*J*<sub>HH</sub> = 7.6 Hz, 2H, *o*-Ph), 6.26 (d, <sup>3</sup>*J*<sub>HH</sub> = 7.5 Hz, 2H, *o*-Ph), 6.50 (t, <sup>3</sup>*J*<sub>HH</sub> = 7.3 Hz, 1H, *p*-Ph), 6.66 (t, <sup>3</sup>*J*<sub>HH</sub> = 7.2 Hz, 1H, *p*-Ph), 6.77 (t, <sup>3</sup>*J*<sub>HH</sub> = 7.5 Hz, 2H, *m*-Ph), 6.86 (t, <sup>3</sup>*J*<sub>HH</sub> = 7.4 Hz, 2H, *m*-Ph). <sup>13</sup>C{<sup>1</sup>H} NMR (100 MHz, 23 °C, benzene-*d*<sub>6</sub>): δ 13.48 (Cp-Me), 15.36 (Cp-Me), 16.81 (Ar-Me), 16.95 (Ar-Me), 17.89 (Ar-Me), 18.66 (Ar-Me), 30.70 (C<sub>2</sub>H<sub>4</sub>), 64.71 (CH<sub>2</sub>Ph), 69.41 (CH<sub>2</sub>Ph), 110.57 (Ar), 115.81 (Ar), 120.95 (*p*-Ph), 121.85 (*p*-Ph), 125.55 (Ar), 126.36 (Ar), 127.18 (*o*-Ph), 127.20 (*m*-Ph), 127.68 (Ar), 127.94 (*m*-Ph), 128.65 (*o*-Ph), 129.03 (Ar), 129.56 (Ar), 132.32 (Ar), 133.32 (Ar), 151.39 (*i*-Ph), 151.63 (*i*-Ph). Unit cell data: monoclinic, *P*2<sub>1</sub>/*n*, *a* = 12.1915(3), *b* = 19.1827(4), *c* = 15.3626(3), α = γ = 90°, β = 93.2526(18). CCDC: 1451241. MS (EI): found 726.2760; calculated 726.3198. Major fragmentation peaks noted at 635, 544 and 91 corresponding to [(EBI\*)Zr(CH<sub>2</sub>Ph)]<sup>+</sup>, [(EBI\*)Zr]<sup>+</sup> and [(CH<sub>2</sub>Ph)]<sup>+</sup> respectively. IR (KBr) (cm<sup>−1</sup>): 2962, 1738, 1543, 1434, 1374, 1261, 1205, 1094, 1022, 802, 668.

### 2.2.2. Preparation of *meso*-(EBI\*)Zr(CH<sub>2</sub><sup>*i*</sup>Bu)Cl

A solution of Li(CH<sub>2</sub><sup>t</sup>Bu) (53.5 mg, 0.69 mmol) in benzene (10 mL) was added to a Schlenk tube containing *meso*-(EBI\*)ZrCl<sub>2</sub> (200 mg, 0.34 mmol) in benzene (40 mL). The reaction mixture was stirred for 1 h before drying under reduced pressure to yield a pale orange solid. Extraction into hexane and subsequent removal of the volatiles *in vacuo* afforded *meso*-(EBI\*)Zr(CH<sub>2</sub><sup>t</sup>Bu)Cl as a pale orange powder in 21% yield (44.5 mg, 0.07 mmol). Very small, pale orange crystalline blocks were grown from a hexane solution at –35 °C. <sup>1</sup>H NMR (400 MHz, 23 °C, benzene-*d*<sub>6</sub>): δ –2.23 (s, 2H, CH<sub>2</sub><sup>t</sup>Bu), 0.74 (s, 9H, CMe<sub>3</sub>), 1.92 (s, 6H, Cp-Me), 2.07 (s, 6H, Ar-Me), 2.14 (s, 6H, Ar-Me), 2.44 (s, 6H, Ar-Me), 2.47 (s, 6H, Ar-Me), 2.53 (s, 6H, Ar-Me), 3.16 (m, 3.10–3.25, 2H, CH<sub>2</sub>), 3.63 (m, 3.56–3.69, 2H, CH<sub>2</sub>). <sup>13</sup>C{<sup>1</sup>H} NMR (100 MHz, 23 °C, benzene-*d*<sub>6</sub>): δ 14.06 (Ar-Me), 16.30 (Ar-Me), 16.77 (Ar-Me), 16.86 (Ar-Me), 17.71 (Ar-Me), 18.81 (Ar-Me), 30.86 (CH<sub>2</sub>), 34.95 (CMe<sub>3</sub>), 77.24 (CH<sub>2</sub><sup>t</sup>Bu), 111.79 (Cp), 116.90 (Cp), 125.22 (Ar), 127.53 (Ar), 127.95 (Ar), 129.50 (Cp), 130.27 (Ar), 132.47 (Ar), 133.72 (Ar). Unit cell data: triclinic, *P* $\bar{1}$ , *a* = 11.4222(5), *b* = 15.9204(6), *c* = 19.5395(7), α = 92.805(3), β = 90.490(3), γ = 108.372(4). CCDC: 1451242. MS (EI): no molecular ion peak was found. Major fragmentation peaks at 592 and 551, corresponding to [(EBI\*)Zr(CH<sub>2</sub><sup>t</sup>Bu)]<sup>+</sup> and [(EBI\*)ZrCl]<sup>+</sup> respectively. IR (KBr) (cm<sup>–1</sup>): 3386 (b), 2962, 1640, 1459, 1261, 1095, 1020, 801.

### 2.3. Polymerisation study

#### 2.3.1. Preparation of polymethylaluminoxane-supported zirconocene catalysts

The quantity of catalyst immobilised on the surface of the support is given in terms of the Al:Zr ratio of the polymethylaluminoxane component to the organometallic complex. This was typically 300:1. In the glovebox, the support and the complex were weighed out into a Schlenk tube. Toluene (50 mL) was added and the reaction mixture swirled at 60 °C for 1 h. The coloured solid was allowed to settle from the clear, colourless solution which was decanted, and the solid dried *in vacuo* (40 °C, 1 × 10<sup>–2</sup> mbar).

#### 2.3.2. Ethylene polymerisation procedure

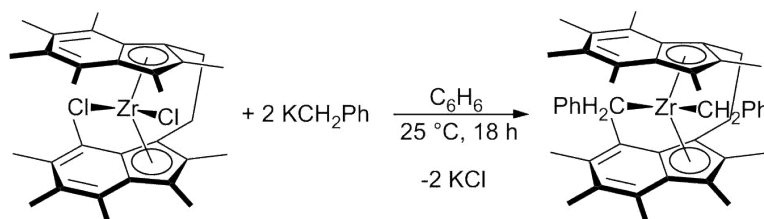
A typical slurry-phase laboratory polymerisation run was performed as follows: TIBA (150 mg) was added to a 150 mL Rotaflo ampoule containing a stirrer bar and rinsed in with hexane (10 mL). The supported complex (10 mg) was added to the

ampoule and washed in with a further hexane (40 mL). The vessel was sealed and was degassed under reduced pressure. The reaction was brought to temperature using an oil bath and the stirring speed was set at 1000 rpm. The stopcock was opened to ethylene at a pressure of 2 bar. On completion of the run, the vessel was closed to ethylene and degassed, before filtration through a glass sintered frit (porosity 3) and washing with pentane (50 mL). The resultant polymer was dried in the vacuum oven at 50 °C overnight.

### 3. Results and discussion

#### 3.1 Synthesis and characterisation of *meso*-(EBI\*)Zr(CH<sub>2</sub>Ph)<sub>2</sub>

*meso*-(EBI\*)Zr(CH<sub>2</sub>Ph)<sub>2</sub> was prepared by addition of benzene directly to a mixture of *meso*-(EBI\*)ZrCl<sub>2</sub> and KCH<sub>2</sub>Ph, followed by stirring at room temperature for 18 hours. After work-up, *meso*-(EBI\*)Zr(CH<sub>2</sub>Ph)<sub>2</sub> was obtained as a yellow microcrystalline solid in 64% yield, Scheme 1.



**Scheme 1.** Synthesis of *meso*-(EBI\*)Zr(CH<sub>2</sub>Ph)<sub>2</sub>.

Crystals of *meso*-(EBI\*)Zr(CH<sub>2</sub>Ph)<sub>2</sub> suitable for an X-ray diffraction study were grown from hexane at -35 °C (Figure 1). *meso*-(EBI\*)Zr(CH<sub>2</sub>Ph)<sub>2</sub> was found to crystallise in the monoclinic spacegroup *P*2<sub>1</sub>/*n*. The value for torsion angle (TA')<sup>†</sup> agrees well with that measured for *meso*-EBI\*ZrCl<sub>2</sub> (18.97°),[23] suggesting either that the benzyl groups have a small effect on the molecular geometry or that the bridge exercises considerable constraint. Another feature is the way that the methyls on the five membered rings splay back, away from the centroid and the plane of the ring by 8.09-14.12° with the largest effect close to the benzyl groups (14.12°). These values match well with *meso*-EBI\*ZrCl<sub>2</sub> where the range is 4.77-10.37°.[23]

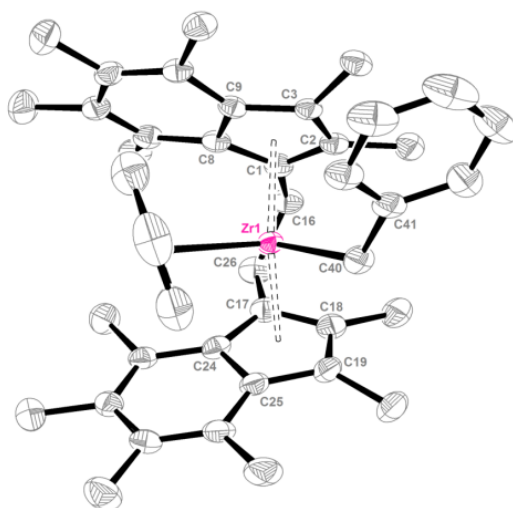


**Figure. 1.** Solid-state molecular structure of *meso*-(EBI\*)Zr(CH<sub>2</sub>Ph)<sub>2</sub>. Hydrogen atoms omitted for clarity. Thermal ellipsoids drawn at 50%.

The value for the tilt angle ( $\alpha$ )<sup>†</sup> of 61.85° significantly exceeds that reported for *meso*-(EBI\*)ZrCl<sub>2</sub> (56.87°), likely to be because of the increased steric bulk of the benzyl groups compared to the chloride. The average Zr-Cp<sub>cent</sub> distance (2.299 Å) for *meso*-(EBI\*)Zr(CH<sub>2</sub>Ph)<sub>2</sub> is marginally longer than for *meso*-EBI\*ZrCl<sub>2</sub> (2.248 Å) and *rac*-(SBI\*)ZrCl<sub>2</sub> (2.250 Å).<sup>[18,23]</sup> Other reported indenyl benzyl compounds, such as (EBTHI)Zr(CH<sub>2</sub>Ph)<sub>2</sub> (EBTHI = ethylenebis(1-tetrahydroindenyl)) and Ind<sup>R</sup><sub>2</sub>Zr(CH<sub>2</sub>Ph)<sub>2</sub> (Ind<sup>R</sup> = 4,7-F<sub>2</sub>-Ind) exhibit slightly shorter Zr-Cp<sub>cent</sub> distances (2.226 and 2.254 Å respectively) indicating that the steric effects dominate the electronic ones in *meso*-(EBI\*)Zr(CH<sub>2</sub>Ph)<sub>2</sub>.<sup>[24-26]</sup> The zirconium benzyl distances (2.335(4) and 2.322(3) Å) are in good agreement with those in the literature,<sup>[27-29]</sup> and match most closely with the only other *ansa*-indenyl benzyl compound reported: (EBTHI)Zr(CH<sub>2</sub>Ph)<sub>2</sub> (2.314 Å).<sup>[27]</sup> Similarly, the twist of the two phenyl rings relative to one another (89.35°) in *meso*-(EBI\*)Zr(CH<sub>2</sub>Ph)<sub>2</sub> falls within the typical range (approximately 70-90°).<sup>[27,28]</sup>

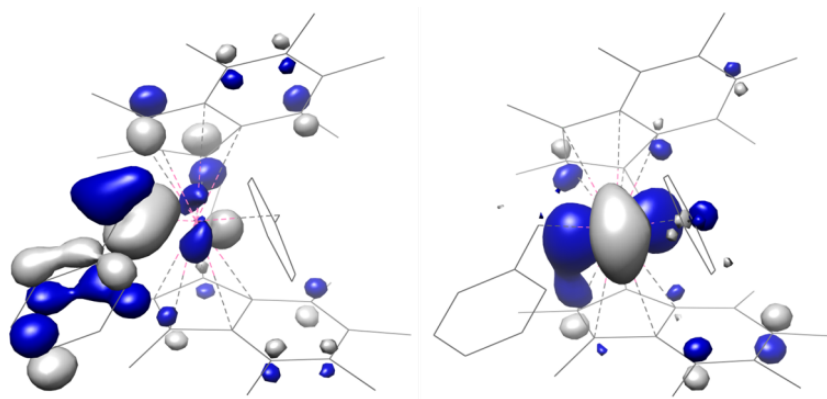


**Figure 2.** Illustration of the DFT-computed HOMO (left) and LUMO (right) of *meso*-(EBI\*)Zr(CH<sub>2</sub>Ph)<sub>2</sub> at the BP86 level.

The DFT studies at both the BP86 and the B3LYP levels corroborate the crystal data, fitting the geometry optimisation well (Figure 2 and Table 1). Analysis of the HOMO shows a bonding interaction between Zr(1) and C(40). Additionally there is significant electron density on the phenyl ring of the same benzyl group, primarily in the  $p_z$  orbitals.

**Table 1.**

Comparison of selected bond lengths (Å), angles (°) and geometric parameters (°) between the crystal structure of *meso*-(EBI\*)Zr(CH<sub>2</sub>Ph)<sub>2</sub> and DFT geometry optimisations.

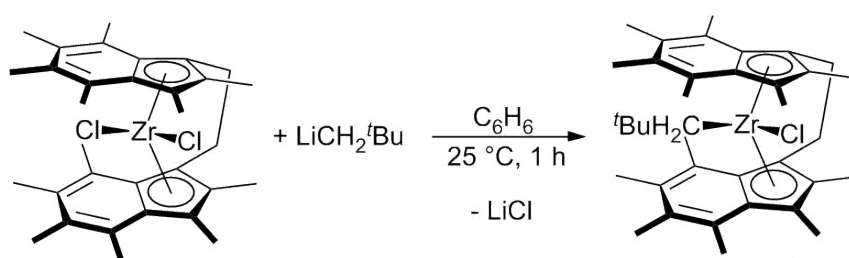
| Bond (Å)/ Angle (°)        | Crystal | B3LYP  | BP86   |
|----------------------------|---------|--------|--------|
| Avg. Zr-Cp <sub>cent</sub> | 2.299   | 2.363  | 2.337  |
| Avg. Zr-C(33)/(40)         | 2.328   | 2.341  | 2.344  |
| Zr(1)-C(33)-C(34)          | 119.49  | 124.10 | 119.21 |
| Zr(1)-C(40)-C(41)          | 128.85  | 129.05 | 131.30 |
| $\alpha$                   | 61.85   | 62.92  | 63.17  |

The <sup>1</sup>H NMR spectrum of *meso*-(EBI\*)Zr(CH<sub>2</sub>Ph)<sub>2</sub> (Figure S4) contains the same diagnostic ligand resonances as *meso*-EBI\*ZrCl<sub>2</sub>;[23] six singlets between 1.85-2.70 ppm, each of intensity six and two of which are coincident (2.04 ppm). The bridge protons are observed as two quartets, each of intensity two, in the range 3-4 ppm. Two singlets at 1.83 and -0.70 ppm which were attributed to the benzylic CH<sub>2</sub> protons. A variable temperature NMR spectroscopic study was carried out on *meso*-(EBI\*)Zr(CH<sub>2</sub>Ph)<sub>2</sub> in tetrahydrofuran-*d*<sub>8</sub> from 193 to 293 K (Figure S6). The

rotation of the phenyl rings was not seen to slow on the NMR spectroscopic timescale, as evidenced by the singlets corresponding to the benzylic protons seen at 193 K. Similarly, six resonances for the phenyl rings are seen to remain, maintaining their respective multiplicities although their relative chemical shifts change. A rotating-frame nuclear Overhauser effect spectroscopy (ROESY) experiment was also conducted (Figure S7) and demonstrates that one pair of benzylic protons lies directly between the two arenes (Figure S8) and may be affected by the ring currents.[30] Attempts to synthesise the related mono-benzyl complex, *meso*-(EBI\*)Zr(CH<sub>2</sub>Ph)Cl, were unsuccessful; analysis of the reaction mixtures by <sup>1</sup>H NMR spectroscopy indicated only the presence of *meso*-(EBI\*)Zr(CH<sub>2</sub>Ph)<sub>2</sub> and *meso*-(EBI\*)ZrCl<sub>2</sub>.

### 3.2 Synthesis and characterisation of *meso*-(EBI\*)Zr(CH<sub>2</sub><sup>*t*</sup>Bu)Cl.

Addition of one equivalent of lithium neopentyl to *meso*-(EBI\*)ZrCl<sub>2</sub> showed no reaction, except for the formation of neopentane, while two equivalents generated *meso*-(EBI\*)Zr(CH<sub>2</sub><sup>*t*</sup>Bu)Cl. The addition of more Li(CH<sub>2</sub><sup>*t*</sup>Bu) provoked no further reaction, but caused the mono-neopentyl complex to decompose. The use of the less basic (CH<sub>2</sub><sup>*t*</sup>Bu)MgCl did not change the reactivity and the bis(neopentyl) complex was not synthesised. In both cases, *meso*-(EBI\*)Zr(CH<sub>2</sub><sup>*t*</sup>Bu)Cl was found to be decomposing in solution at room temperature over the course of 48 hours. Accordingly, two equivalents of Li(CH<sub>2</sub><sup>*t*</sup>Bu) and one of *meso*-(EBI\*)ZrCl<sub>2</sub> were allowed to stir for one hour in benzene (Scheme 2).



**Scheme 2.** Synthesis of *meso*-(EBI\*)Zr(CH<sub>2</sub><sup>*t*</sup>Bu)Cl.

Single crystals suitable for an X-ray diffraction study were obtained after four days at −30 °C (Figure 3).



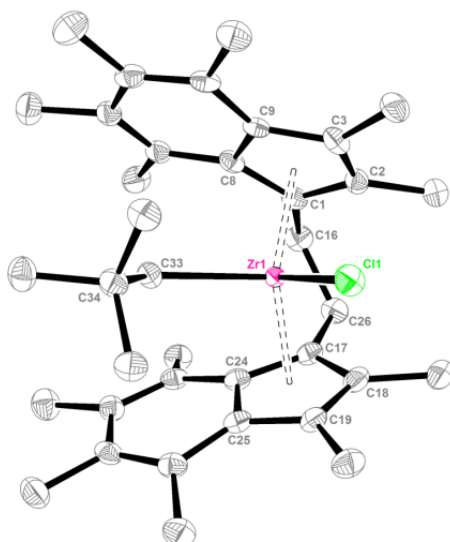


**Fig. 3.** Solid-state molecular structure of *meso*-(EBI\*)Zr(CH<sub>2</sub><sup>t</sup>Bu)Cl (isomer 1 shown). Hydrogen atoms omitted for clarity. Thermal ellipsoids drawn at 50%.

Two molecules of *meso*-(EBI\*)Zr(CH<sub>2</sub><sup>t</sup>Bu)Cl and 1 molecule of hexane crystallised in the asymmetric unit, labelled 1 and 2 in Fig. S2. The average zirconium-centroid distance (2.286 Å) reported for *meso*-(EBI\*)Zr(CH<sub>2</sub><sup>t</sup>Bu)Cl (isomer 1) agrees well with that of both *meso*-(EBI\*)ZrCl<sub>2</sub> (2.248 Å) and *meso*-(EBI\*)Zr(CH<sub>2</sub>Ph)<sub>2</sub> (2.299 Å).[23] The Zr(1)-C(33) distance in *meso*-(EBI\*)Zr(CH<sub>2</sub><sup>t</sup>Bu)Cl (2.293(3) Å) agrees well with that for the other structurally characterised zirconocene neopentyl chloride (2.3258(12) and 2.3287(12) Å for the two isomers) as well as with other zirconium neopentyl bonds in the literature (2.256-2.352 Å).[31-33] It also matches very closely to the Zr(1)-C(33) and Zr(1)-C(40) bond distances reported for *meso*-(EBI\*)Zr(CH<sub>2</sub>Ph)<sub>2</sub> (2.325(4) and 2.322(3) Å). The tilt angle (60.49°) is intermediary between *meso*-(EBI\*)ZrCl<sub>2</sub> (56.87°) and *meso*-(EBI\*)Zr(CH<sub>2</sub>Ph)<sub>2</sub> (61.85°) and the value for TA' (20.11°) shows the rings in *meso*-(EBI\*)Zr(CH<sub>2</sub><sup>t</sup>Bu)Cl to be close to eclipsed as in *meso*-(EBI\*)ZrCl<sub>2</sub> (18.97°) and *meso*-(EBI\*)Zr(CH<sub>2</sub>Ph)<sub>2</sub> (17.42°).

DFT studies were undertaken for *meso*-(EBI\*)Zr(CH<sub>2</sub><sup>t</sup>Bu)Cl and a comparison of the pertinent bond angles is given in Table 2. Both basis sets do lengthen all contacts with the zirconium very slightly as well as increasing the value of  $\alpha$  by approximately 2°. The calculated HOMO is predominantly based on the indenyl ligand, the LUMO is significantly based on the metal, as in all the reported d<sup>0</sup> zirconocenes, with 43.7% of the electron density based on the Zr d<sub>xy</sub> orbital, Fig. 4.

**Table 2.**

Comparison of selected bond lengths (Å), angles (°) and geometric parameters (°) between the crystal structure of *meso*-(EBI\*)Zr(CH<sub>2</sub><sup>*t*</sup>Bu)Cl and DFT geometry optimisations using two basis sets: B3LYP and BP86.

| Bond (Å)/ Angle (°)        | Crystal     | B3LYP       | BP86        |
|----------------------------|-------------|-------------|-------------|
| Avg. Zr-Cp <sub>cent</sub> | 2.286       | 2.349       | 2.329       |
| Zr(1)-C(33)                | 2.293(3)    | 2.318       | 2.319       |
| Zr(1)-Cl(1)                | 2.4365(8)   | 2.454       | 2.448       |
| Δ <sub>M-C</sub> (Å)       | 0.253/0.125 | 0.164/0.134 | 0.158/0.137 |
| Zr(1)-C(33)-C(34)          | 128.3(2)    | 127.41      | 127.42      |
| α                          | 60.49       | 62.81       | 62.23       |

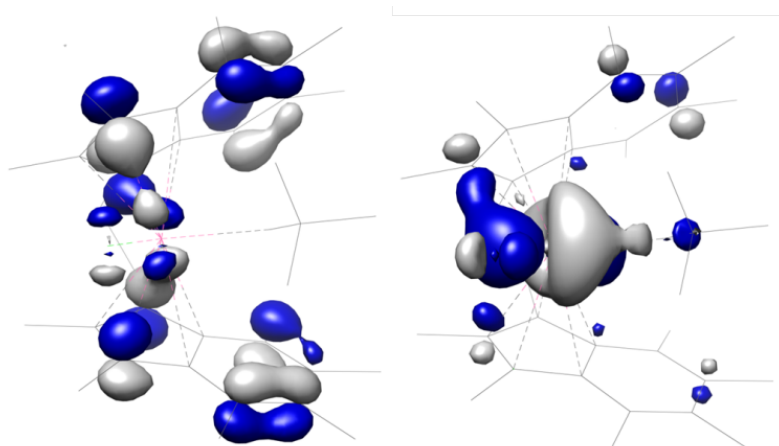


**Fig. 4.** Illustration of the DFT computed HOMO (left) and LUMO (right) of *meso*-(EBI\*)Zr(CH<sub>2</sub><sup>*t*</sup>Bu)Cl at the B3LYP level.

The <sup>1</sup>H NMR spectrum of *meso*-(EBI\*)Zr(CH<sub>2</sub><sup>*t*</sup>Bu)Cl in benzene-*d*<sub>6</sub> has an extremely shielded methylene group (−2.23 ppm) and a resonance with intensity nine (0.74 ppm) corresponding to the *tert*-butyl group of the neopentyl. Six methyl singlets fall in the range 1.91-2.53 ppm and the bridge multiplets are seen at 3.17 and 3.63 ppm. Co-crystallised hexane is also observed in the spectrum, Fig S9.

### 3.3 Synthesis of polymethylaluminumoxane supported zirconocene catalysts

*Meso*-(EBI\*)Zr(CH<sub>2</sub>Ph)<sub>2</sub> or *meso*-(EBI\*)Zr(CH<sub>2</sub><sup>*t*</sup>Bu)Cl were added to a slurry of solid polymethylaluminumoxane (sMAO) in toluene and heated to 60 °C for 60 minutes, the solution became colourless and the solid polymethylaluminumoxane took on a pink

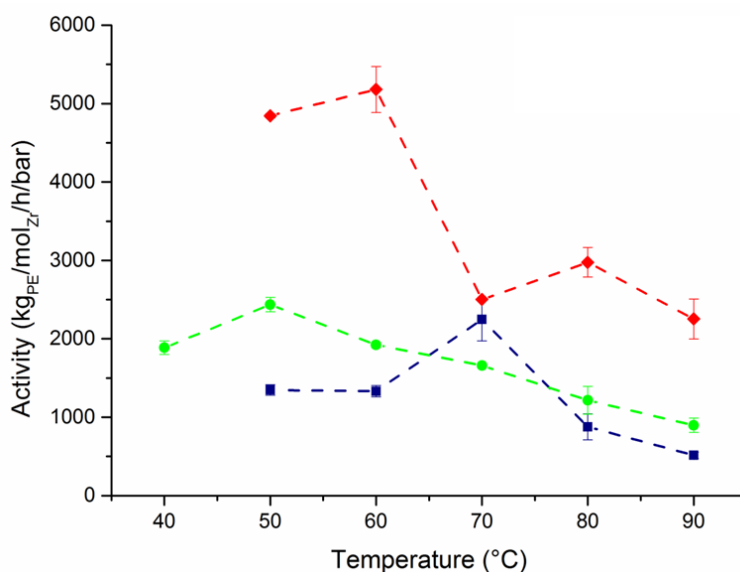
colour. The Al:Zr ratio in the finished solid catalyst was estimated at 300 based on complete immobilisation of the zirconocene on the sMAO. Solid polymethylaluminoxane (sMAO) is a polymeric, porous aluminoxane that is a solid, insoluble form of MAO suitable for supporting catalysts.[34] The structure, like MAO, is poorly defined, and efforts within the group are currently ongoing to better understand this material

### 3.4 Slurry phase ethylene polymerisation

Slurry phase ethylene polymerisation reactions were carried out in a 150 mL glass batch reactor under 2 bar ethylene in hexane. Typically 150 mg TIBA was added to 50 mL hexane and 10 mg supported catalyst.

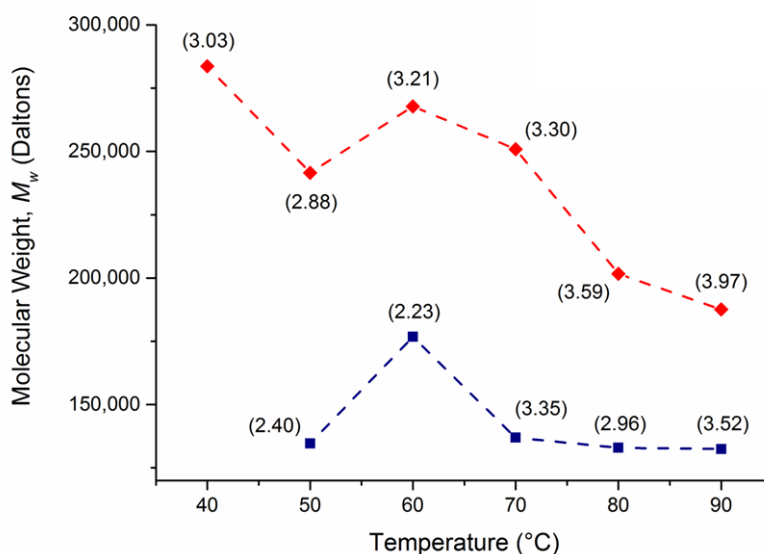
sMAO/*meso*-(EBI\*)Zr(CH<sub>2</sub>Ph)<sub>2</sub> showed the optimum activity two times higher (5,179 kg<sub>PE</sub>/mol<sub>Zr</sub>/h/bar) than sMAO/*meso*-(EBI\*)Zr(CH<sub>2</sub><sup>t</sup>Bu)Cl and sMAO/*meso*-(EBI\*)ZrCl<sub>2</sub> (2,436 and 2,246 kg<sub>PE</sub>/mol<sub>Zr</sub>/h/bar respectively), Fig. 5.

Fig. 6 illustrates the molecular weight data of the polyethylene (PE) produced by sMAO/*meso*-(EBI\*)Zr(CH<sub>2</sub>Ph)<sub>2</sub> and sMAO/*meso*-(EBI\*)Zr(CH<sub>2</sub><sup>t</sup>Bu)Cl. The molecular weights of the PE produced by sMAO/*meso*-(EBI\*)Zr(CH<sub>2</sub><sup>t</sup>Bu)Cl are higher at all temperatures (above 188 000 kg/mol; 90 °C) than those for sMAO/*meso*-(EBI\*)Zr(CH<sub>2</sub>Ph)<sub>2</sub> (176 708 kg/mol; 60 °C). The GPC traces are shown in Figures S12 and S13 and highlight strictly unimodal characteristics.



**Fig. 5.** Temperature dependence of the ethylene polymerisation activity for sMAO/ *meso*-EBI\*ZrCl<sub>2</sub> (blue square), sMAO/ *meso*-(EBI\*)Zr(CH<sub>2</sub>Ph)<sub>2</sub> (red diamond) and sMAO/ *meso*-(EBI\*)Zr(CH<sub>2</sub><sup>t</sup>Bu)Cl

(green circle). Polymerisation conditions:  $[Al]_0:[Zr]_0 = 300:1$ . 150 mg TIBA scavenger, 2 bar ethylene, 10 mg catalyst, 50 mL hexane and 30 minutes.



**Fig. 6.** Temperature dependence of the molecular weights,  $M_w$ , of the polyethylene produce by sMAO/*meso*-(EBI\*)Zr(CH<sub>2</sub>Ph)<sub>2</sub> (blue square) and sMAO/ *meso*-(EBI\*)Zr(CH<sub>2</sub><sup>t</sup>Bu)Cl (red diamond). The polyethylene polydispersities ( $M_w/M_n$ ) are given in parentheses. Polymerisation conditions:  $[Al]_0:[Zr]_0 = 300:1$ . 150 mg TIBA scavenger, 2 bar ethylene, 10 mg catalyst, 50 mL hexane and 30 minutes.

Following our recent publication on the use of *rac*-(EBI\*)ZrCl<sub>2</sub> supported on silica and aqueous miscible organic layered double hydroxides (AMO-LDHs),[18] we are now expanding our scope to a polymethylaluminoxane support.

Fig. S10 compares the activity data for *rac*-(EBI\*)ZrCl<sub>2</sub> supported on methylaluminoxane derived silica (SSMAO) and polymethylaluminoxane (sMAO). The activity for polymethylaluminoxane sMAO/ *rac*-(EBI\*)ZrCl<sub>2</sub> peaks at 50 °C (5,365 kg<sub>PE</sub>/mol<sub>Zr</sub>/h/bar) – more than three times that of the silica analogue at the same temperature (1,649 kg<sub>PE</sub>/mol<sub>Zr</sub>/h/bar). Activities from 50-70 °C remain in excess of 4500 kg<sub>PE</sub>/mol<sub>Zr</sub>/h/bar. System based on Cp<sub>2</sub>ZrCl<sub>2</sub> and Cp<sub>2</sub>'ZrCl<sub>2</sub> (Cp' = C<sub>5</sub>H<sub>4</sub>Me) and (EBTHI)ZrCl<sub>2</sub> show activities of 5,400, 9180 and 4,320 kg<sub>PE</sub>/mol<sub>Zr</sub>/h/bar (all at 60 °C) respectively.[35,36] These values compare excellently with those shown in Fig. S10 although they require an MAO scavenger. The molecular weights for *rac*-(EBI\*)ZrCl<sub>2</sub> supported on polymethylaluminoxane is described in Fig. 7 and shows a general decrease with increasing temperature from 180,000 to 115,000 kg/mol (40 to 90 °C

respectively). These values are consistently lower than the equivalent results on SSMAO,[18] the polydispersities remain almost constant across the temperature range (approximately 2.5). The GPC traces are shown in Figure S14 and highlights strictly unimodal characteristics.

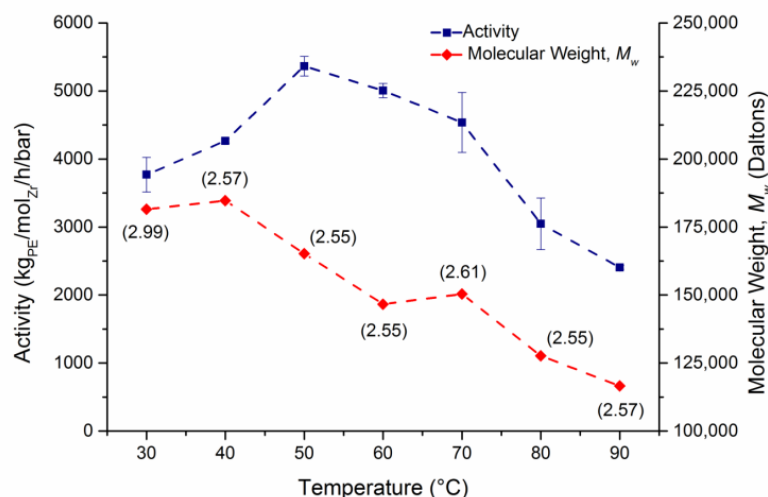


**Fig. 7.** Temperature dependence of ethylene polymerization activity (blue square) and  $M_w$  (red diamond), for s-MAO/*rac*-(EBI\*)ZrCl<sub>2</sub>. The polyethylene polydispersities ( $M_w/M_n$ ) are given in parentheses. Polymerisation conditions: [Al]<sub>0</sub>: [Zr]<sub>0</sub> = 200:1. 150 mg TIBA scavenger, 2 bar ethylene, 10 mg catalyst, 50 mL hexane and 30 minutes.

Ransom *et al.* demonstrated that *rac*-(EBI\*)ZrCl<sub>2</sub> outperforms *meso*-(EBI\*)ZrCl<sub>2</sub> in solution by a factor of 1.6 (38,300 to 61,800 kg<sub>PE</sub>/mol<sub>Zr</sub>/h/bar at 80 °C).[23] This discrepancy is exaggerated in the catalysts supported on solid polymethylaluminoxane where the differential is above 3.5. It is perhaps interesting to note that while *meso*-(EBI\*)ZrCl<sub>2</sub> shows an optimum activity at 70 °C (2,246 kg<sub>PE</sub>/mol<sub>Zr</sub>/h/bar), *rac*-(EBI\*)ZrCl<sub>2</sub> peaks at only 50 °C (5,365 kg<sub>PE</sub>/mol<sub>Zr</sub>/h/bar).

A series of olefin pre-catalysts were supported on solid polymethylaluminoxane and the results are collated in Table 3.

**Table 3.**

Summary of the slurry phase polymerisation of ethylene using solid polymethylaluminoxane (sMAO) supported olefin pre-catalysts.

| Catalysts  | [Al] <sub>0</sub> /[Zr] <sub>0</sub> | Activity<br>(kg <sub>PE</sub> /mol <sub>Zr</sub> /h/bar) | Ref.       |
|--|--------------------------------------|--|------------|
| sMAO/ <i>rac</i> -(EBI)ZrCl <sub>2</sub>   | 200                                  | 6,533  | -          |
| sMAO/ <i>rac</i> -(EBI*)ZrCl <sub>2</sub>  | 200                                  | 5,006  | this paper |
| sMAO/ <i>meso</i> -(EBI*)ZrCl <sub>2</sub>   | 300                                  | 1,331  | this paper |
| sMAO/ <i>meso</i> -(EBI*)Zr(CH <sub>2</sub> Ph) <sub>2</sub>                           | 300                                  | 5,179  | this paper |
| sMAO/ <i>meso</i> -(EBI*)Zr(CH <sub>2</sub> <sup>t</sup> Bu)Cl                         | 300                                  | 1,923  | this paper |
| sMAO/ <i>rac</i> -(SBI*)ZrCl <sub>2</sub>  | 300                                  | 5,971  | -          |
| sMAO/ <i>rac</i> -(Ind <sup>#</sup> ) <sub>2</sub> ZrCl <sub>2</sub>                   | 300                                  | 870  | -          |
| sMAO/ <i>rac</i> -(Ind <sup>#</sup> ) <sub>2</sub> Zr(CH <sub>2</sub> Ph) <sub>2</sub> | 300                                  | 1,063  | -          |
| sMAO/ <i>meso</i> -(Ind <sup>#</sup> ) <sub>2</sub> ZrCl <sub>2</sub>                  | 300                                  | 343  | -          |
| sMAO/ Pn*ZrCpCl  | 200                                  | 4,209  | 22b        |
| sMAO/ Pn*ZrCp <sup>Me<sup>3</sup></sup> Cl   | 200                                  | 4,096  | 22b        |

Polymerisation conditions: 60 °C, 150 mg TIBA scavenger, 2 bar ethylene, 10 mg catalyst, 50 mL hexane and 30 minutes. (Ind<sup>#</sup>): hexamethylindenyl, (Pn\*): permethylpentalene.

#### 4. Conclusions

We have reported the synthesis of two new ethylene bridged permethylindenyl zirconocene complexes. These compounds were fully characterised by X-ray crystallography and in-depth NMR spectroscopy, including variable temperature and ROESY experiments.

Slurry phase polymerisation of ethylene were carried out using solid catalysts based on these complexes supported on solid polymethylaluminoxane (sMAO). sMAO/*meso*-(EBI\*)Zr(CH<sub>2</sub>Ph)<sub>2</sub> showed an optimum activity (5,179 kg<sub>PE</sub>/mol<sub>Zr</sub>/h/bar) that is two times higher than sMAO/*meso*-(EBI\*)Zr(CH<sub>2</sub><sup>t</sup>Bu)Cl (2,436 kg<sub>PE</sub>/mol<sub>Zr</sub>/h/bar). Both sMAO/*meso*-(EBI\*)Zr(CH<sub>2</sub>Ph)<sub>2</sub>, and sMAO/*meso*-EBI\*ZrCl<sub>2</sub> show these optimum activities at 70 and 50 °C respectively. The catalyst activities when solid polymethylaluminoxane (sMAO) was used as a support were three times higher than when SSMAO was used.

#### Acknowledgements

The authors would like to thank SCG Chemicals Co., Ltd, Thailand for funding (T.A.Q.A., Z.R.T. and J.-C.B.) and GPC characterisations. Z.R.T. thanks Trinity

College Oxford for a Junior Research Fellowship. Dr. Alexander (Sandy) Kilpatrick (University of Oxford) is thanked for the polymethylaluminumoxane synthesis.

## Appendix A. Supplementary data

Supplementary data related to this article can be found <http://> This contains: extensive NMR spectroscopy, X-ray crystallography, and polymerisation data.

## Notes

†Definitions of structural parameters are defined in the supporting information (Figs. S15 and S16).

## References

- [1] G. Wilkinson and J. M. Birmingham, *J. Am. Chem. Soc.* 76 (1954) 4281.
- [2] (a) J. A. Pool, E. Lobkovsky and P. J. Chirik, *Nature* 427 (2004) 527; (b) P. J. Chirik, *Dalton Trans* (2007) 16.
- [3] (a) G. W. Margulieux, S. P. Semproni, P. J. Chirik *Angew. Chem. Int. Ed.* 53 (2014) 9189; (b) S. P. Semproni, P. J. Chirik *J. Am. Chem. Soc.* 135 (2013) 11373; (c) D. J. Knobloch, E. Lobkovsky, P. J. Chirik *Nat. Chem.* 2 (2010) 30.
- [4] A. M. Chapman, M. F. Haddow and D. F. Wass, *J. Am. Chem. Soc.* 133 (2011) 18463.
- [5] X. Xu, G. Kehr, C. G. Daniliuc and G. Erker, *Angew. Chemie* 125 (2013) 13874.
- [6] X. Xu, G. Kehr, C. G. Daniliuc and G. Erker *J. Am. Chem. Soc.* 136 (2014) 12431.
- [7] O. G. Piringer and A. L. Baner, *Plastic Packaging: Interactions with Food and Pharmaceuticals*; 2nd Ed.; Wiley, 2008.
- [8] G. J. P Britovsek, V. C. Gibson and D. F. Wass, *Angew. Chem. Int. Ed.* 38 (1999) 428.
- [9] E. Y. Chen and T. J. Marks, *Chem. Rev.* 100 (2000) 1391.
- [10] M. Delferro and T. J. Marks, *Chem. Rev.* 111 (2011) 2450.
- [11] J. R. Severn, J. C. Chadwick, R. Duchateau and N. Friederichs, *Chem. Rev.* 105 (2005) 4073.
- [12] G. G. Hlatky, *Chem. Rev.* 100 (2000) 1347.
- [13] J. R. Severn and J. C. Chadwick, *Taylor-Made Polymers. Via Immobilisation of Alpha-Olefin Polymerization Catalysts*; Wiley-VCH, 2008.

- [14] A. Yano and M. Sato, Olefin polymerization catalyst and olefin polymerization process. US5830820, 1998.
- [15] T. Suzuki and Y. Suga, *Polym. Prepr.* 38 (1997) 207.
- [16] H. Frielingsdorf, H. Müller-Tamm, G. Schweier and L. Reuter, *Inorganic Carriers for Ziegler Catalysts*. DE2163852, 1973.
- [17] Z. P. Xu, J. Zhang, M. O. Adebajo, H. Zhang and C. Zhou, *Appl. Clay Sci.* 53 (2011) 139.
- [18] J.-C. Buffet, T. A. Q. Arnold, Z. R. Turner, P. Angpanitcharoen and D. O'Hare, *RSC Advances* 5 (2015) 87456.
- [19] J.-C. Buffet, N. Wana, T. A. Q. Arnold, E. K. Gibson, P. P. Wells, Q. Wang, J. Tantirungrotechain and D. O'Hare, *Chem. Mater.* 27 (2015) 1495.
- [20] J.-C. Buffet, Z. R. Turner, R. T. Cooper and D. O'Hare, *Polym. Chem.* 6 (2015) 2493.
- [21] J.-C. Buffet, C. F. H. Byles, R. Felton, C. Chen and D. O'Hare, *Chem. Commun.* 52 (2016) 4076.
- [22] (a) C. M. R. Wright, Z. R. Turner, J.-C. Buffet and D. O'Hare, *Chem. Commun.* 52 (2016) 2850. (b) D. A. X. Fraser, Z. R. Turner, J.-C. Buffet and D. O'Hare, *Organometallics* (2016) doi:10.1021/acs.organomet.6b00417.
- [23] P. Ransom, A. E. Ashley, N. D. Brown, A. L. Thompson and D. O'Hare, *Organometallics* 30 (2011) 800.
- [24] W. A. Herrmann, J. Rohrmann, E. Herdtweck, W. Spaleck and A. Winter, *Angew. Chem. Int. Ed.* 28 (1989) 1511.
- [25] R. F. Jordan, R. E. LaPointe, N. Baenziger and G. D. Hinch, *Organometallics* 9 (1990) 1539.
- [26] L. J. Irwin, P. D. Zeits, J. H. Reibenspies and S. A. Miller, *Organometallics* 26 (2007) 1129.
- [27] N. Piccolrovazzi, P. Pino, G. Consiglio, A. Sironi and M. Moret, *Organometallics* 9 (1990) 3098.
- [28] D. Veghini, M. W. Day and J. E. Bercaw, *Inorganica Chim. Acta* 280 (1998) 226.
- [29] F.-C. Liu, J. Liu, E. A. Meyers and S. G. Shore, *Inorg. Chem.* 38 (1999) 2169.
- [30] F. Sauriol, J. F. Sonnenberg, S. J. Chadder, A. F. Dunlop-Brière, M. C. Baird, and P. H. M. Budzelaar, *J. Am. Chem. Soc.* 132 (2010) 13357.
- [31] S. B. Klamo, O. F. Wendt, L. M. Henling, M. W. Day, and J. E. Bercaw, *Organometallics* 26 (2007) 3018.



- [32] J. Jeffery, M. F Lappert, N. T. Luong-Thi, M. Webb, J. L. Atwood and W. E. Hunter, J. Chem. Soc. Dalton Trans. (1981) 1593.
- [33] T. Dreier, K. Bergander, E. Wegelius, R. Fröhlich and G. Erker, Organometallics 20 (2001) 5067.
- [34] E. Kaji and E. Yoshioka, Solid polymethylaluminoxane composition and process for producing same, 2010, WO2010055652.
- [35] W. Kaminsky, J. Chem. Soc. Dalton Trans. (1998) 1413
- [36] W. Kaminsky, R. Engehausen, K. Zoumis, W. Spaleck and J. Rohrmann, Makromol. Chem. 193 (1992) 1643.